ACS OMEGA

http://pubs.acs.org/journal/acsodf

Article

Simultaneous Pyrolysis of Coal and Biomass in a Drop-Tube−Fixed-Bed Reactor

Yibo Zhao, Lu Chang, Tingting Huang, Guojun Yin, Wenjing He,* Lanjun Zhang,* Minjie Cui, Shuyue Xu, and Ziheng Liu

Cite This: *ACS Omega* 2022, 7, 8717−8723

Read Online

ACCESS | Metrics & More | Article Recommendations

ABSTRACT: Copyrolysis of coal and biomass has been extensively studied to exploit its inherent synergistic effects; however, the different pyrolysis temperature zones of coal and biomass seriously affect the realization of these effects. Therefore, a new copyrolysis method (preheating the coal to a certain temperature and then adding the biomass in a drop-tube−fixed-bed reactor, denoted as M1) was designed herein to achieve "simultaneous" pyrolysis of coal and biomass. The yields of products and the characteristics of M1-produced tar were estimated and compared with those of tar obtained by fixed-bed-reactor (denoted as M2)-based copyrolysis. M1 achieved a higher tar yield and lower water content than M2. The M1-generated tar exhibited a lower free-radical concentration, higher H/C ratio, higher levels of uncondensed aromatic hydrogen, and shorter side-chains than that produced by M2. The temperature of HLBE coal at which the WSs were fed to the reactor in M1, denoted as T_F, affects the "simultaneous" pyrolysis. T_F values of 300, 400, and 500 °C were studied, and it was found that the tar yield obtained at a T_F of 400 °C (the main pyrolysis temperature of coal) is the highest, the water yield is the lowest, and the free-radical concentration of the tar is also the lowest among the investigated samples.

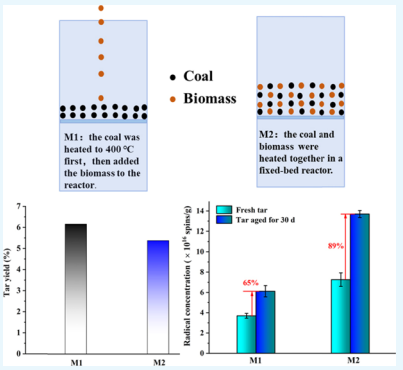

1. INTRODUCTION

Pyrolysis of coal or biomass to produce liquid fuels has been extensively investigated to compensate for the dwindling oil reserves and mitigate the ongoing oil crisis. Copyrolysis of coal and biomass, in comparison with their separate pyrolysis, enables the sustainable development of energy resources. Moreover, biomass is believed to be a hydrogen-rich substance that can be utilized as a hydrogen donor to stabilize large free-radical fragments, radicals with a high molecular weight, produced by coal, and to improve the yield and quality of the resulting liquid product.[1,2] Therefore, copyrolysis of coal and biomass has been comprehensively probed using various types of reactors.[3−5]

In principle, the copyrolysis of coal and biomass follows a free-radical mechanism in which the covalent bonds of the biomass and coal are successively ruptured, which produces free-radical fragments that react further via breakage, binding, or polycondensation to form tar, gases, char, and soot.[6−8] The synergistic effect realized in this copyrolysis is essentially due to the interactions between the free radicals of coal and biomass generated during copyrolysis.[7,9] However, the pyrolysis temperatures of biomass (200−450 °C) and coal (300−600 °C) are different because of their different structures, which causes issues in terms of monitoring this synergistic effect. Additionally, the existence of this synergistic effect has been questioned.[10−12] Theoretically, the synergistic effect should be maximized if the coal and biomass can achieve "simultaneous" pyrolysis during copyrolysis. Therefore, fast copyrolysis with a high heating rate has been employed to enable rapid realization of the pyrolysis temperatures of coal and biomass (in seconds) and the release of a large amount of reactive radical fragments of coal and biomass, which enhance the synergistic effect.[13−15] Zhu et al.[14] conducted fast copyrolysis of a massive Naomaohu coal and cedar mixture using rapid infrared heating and found the existence of synergies from primary volatiles of coal and biomass. Yuan et al.[15] reported that significant synergies can happen during rapid copyrolysis of biomass and coal when they are in close contact. Compared with that of the conventional slow pyrolysis, fast pyrolysis reduces the influence of the different pyrolysis temperatures of the different feedstocks on the synergistic effect of copyrolysis.

Devices such as drop-tube reactors or free-fall reactors,[16,17] drop-tube−fixed-bed reactors,[13] and fluidized-bed reactors[18−20] have been employed to implement rapid copyrolysis.

Received: December 7, 2021
Accepted: February 22, 2022
Published: March 2, 2022

Regardless of the type of reactor, the temperature of the furnace is typically set to extremely high levels (500−1000 °C) to achieve a high heating rate of the copyrolysis. Moreover, the heating furnaces of free-fall reactors are considerably lengthy to ensure sufficient residence time for the complete pyrolysis of samples during falling. Zhang J et al.[16] and Zhang L et al.[3] employed heating furnaces that were 1600 and 1800 mm long and preheated to 700 and 500−700 °C, respectively, in their free-fall reactors. These operations are not only energy- and cost-intensive but also provide poor oil quality because the volatiles generated from the particle surfaces of coal and biomass are subjected to higher ambient temperatures for a long residence time, which increases the degree of the secondary reaction and degrades the quality of the resulting tar.[21]

A new copyrolysis method based on a drop-tube−fixed-bed reactor was developed in the present study to achieve "simultaneous" pyrolysis of coal and biomass. Prior to the experiments, the coal sample was first added to the reactor followed by the addition of biomass from the top of the reactor when the coal was heated to its pyrolysis temperature. The yields and properties of the resulting products were investigated and compared with those obtained using a fixed-bed reactor. In addition, the effects of the feed temperature of the biomass on the yields and properties of the products were examined.

2. RESULTS AND DISCUSSION

2.1. Product Yields Achieved by the Copyrolysis Setups. Figure 1 shows the yields of the products produced by

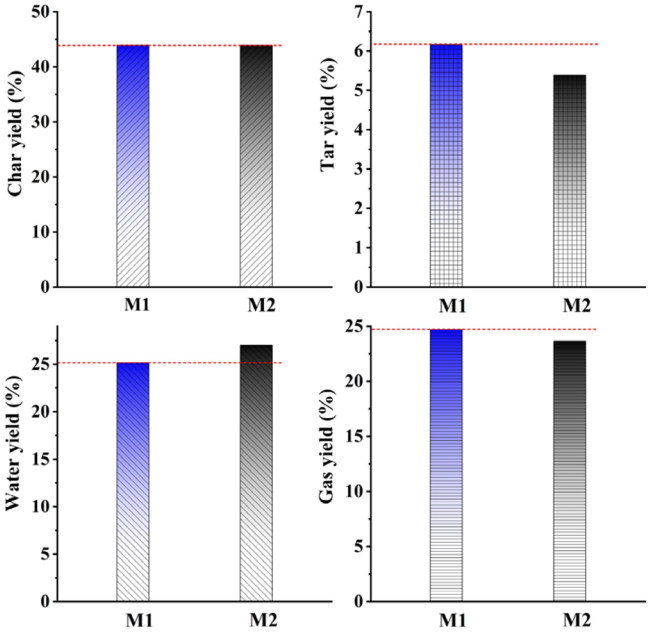

Figure 1. Product yields obtained by the two pyrolysis methods.

the M1 and M2 methods. For M1, the Hulunbeier (HLBE) coal was heated from 25 to 400 °C first, then the walnut shells (WSs) were added to the reactor, and the experiment was terminated at a sample temperature of 600 °C. For M2, the coal and the biomass were heated together from 25 to 600 °C in a fixed-bed reactor. The liquid product of the pyrolysis contains tar and water, whose yields were measured separately. Figure 1 suggests that the char yields produced by M1 and M2 are identical, whereas the yields of tar and gases produced by M1 are higher than those of M2; moreover, the amount of water produced by M1 is lower than that of M2, which indicates that copyrolysis in M1 facilitates the occurrence of synergistic effects.

The process of pyrolysis was subsequently probed to clarify these results. To better understand the pyrolysis process, Figure 2 shows the differential thermogravimetric (DTG)

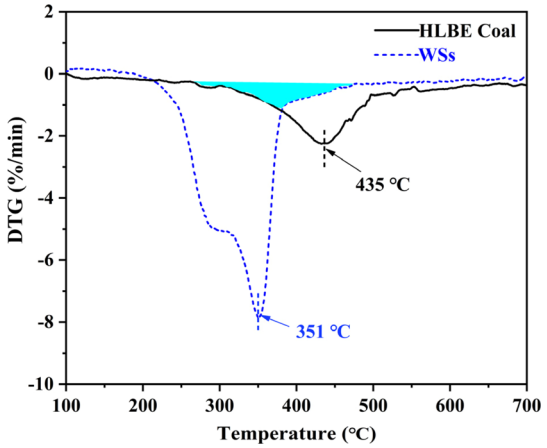

Figure 2. DTG curves of the pyrolysis of HLBE coal and WSs.

curves for HLBE coals and WSs from 100 to 700 °C. From Figure 2, we can see that the peak pyrolysis temperatures of the WSs and HLBE coal are 351 and 435 °C, respectively, with a small overlapping zone of the two profiles (the shaded part in Figure 2). The successive pyrolysis of WSs and HLBE coal in M2 leads to a small overlapping zone of copyrolysis, as shown in Figure 2; therefore, the free-radical fragments from the WSs have a relatively small chance of interacting with those from the HLBE coal. However, in M1, the WSs were added when the temperature of the HLBE coal reached 400 °C, which is close to the peak pyrolysis temperature of HLBE coal, as shown in Figure 2. All the free radicals produced by the pyrolysis of WSs in M1 could combine with those produced by the pyrolysis of coal, resulting in the HLBE coal and WSs being "simultaneously" pyrolyzed to a certain extent, compared to that in M2. This enhances the synergistic effects of the copyrolysis of HLBE coal and the WSs.

2.2. Characteristics of Tar Produced by M1 and M2. *2.2.1. Free-Radical Concentration of Tar.* Copyrolysis follows a free-radical mechanism by which the interactions between the volatile free-radical fragments produced by the two materials affect the free-radical concentration of the produced tar. The free-radical concentration of the tars shown in Figure 3 is an average of three experiments, and the error bars are obtained by calculating the standard deviation (the same below). According to Figure 3, the free-radical concentration of the tar obtained by M1 (3.7×10^{16} spins/g) is significantly lower than that obtained by M2 (7.2×10^{16} spins/g). Additionally, the free-radical concentrations of the M1- and M2-produced tar samples that were placed at 25 °C for 30 d increased by 65 and 89%, respectively.

The concentration of free radicals in tar is proportional to the content of its heavy components,[6,22] with more than 90% of the free radicals in tar originating from its *n*-hexane-insoluble fraction. Therefore, the results shown in Figure 3 indicate that the quality and stability of the tar obtained by M1

https://doi.org/10.1021/acsomega.1c06912
ACS Omega 2022, 7, 8717−8723

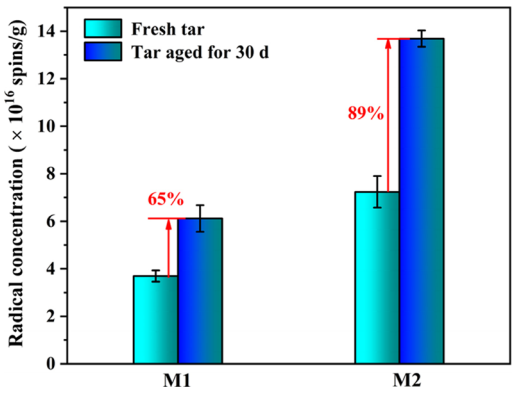

Figure 3. Free-radical concentrations of fresh tar samples and tar samples aged for 30 d.

are superior to those of the tar produced by M2. This is because the free radicals obtained from different materials have more opportunities to combine with each other in M1 than in M2; this leads to the small free radicals produced by the WSs (low-molecular-weight radicals such as $H^{\cdot}$, $OH^{\cdot}$, and CH_3) combining with and stabilizing the radicals produced by HLBE coal, resulting in a reduction in the concentration of free radicals in the M1-produced tar. Because a greater number of free radicals are stabilized during copyrolysis, the M1-produced tar contains fewer radicals than that produced by M2. Radicals are unstable and can react with oxygen in the air, leading to aging of the resulting oil;[23,24] therefore, the M1-produced tar with a low free-radical concentration is more stable than that of M2.

2.2.2. Ultimate and Proton Nuclear Magnetic Resonance Analyses of Tar. The ultimate analysis results of the produced tar are listed in Table 1, which suggest that the H/C ratio of the M1-produced tar (1.32) is higher than that of the M2-generated one (1.27). ^{1}H-NMR analysis of the resulting tar was performed to investigate the distributions of hydrogen. The hydrogens were categorized according to their chemical shifts,[25,26] with each region being integrated and subsequently normalized. Table 2 shows the proton NMR data featuring aromatic (H_{ar}) and aliphatic protons (H_{al}) and the distributions of the tar produced by M1 and M2. The value of H_{ar} of the M1-generated tar (22.6%) is higher than that of the M2-generated tar; moreover, the uncondensed aromatic hydrogen (H_u) fraction of the M1-produced tar is higher than that of the M2-produced tar, whereas the condensed aromatic hydrogen (H_c) component of the M1-produced tar is significantly lower than that of the M2-produced one. These results indicate that the tar produced by M1 is lighter than that produced by M2, which is consistent with the estimated free-radical concentrations of the tar samples. Additionally, the contributions of protons in the β (H_β) and γ (H_γ) positions are smaller than those of M2, which indicates fewer long side-chains in the M1-produced tar.[27]

Table 1. Ultimate Analyses of the Copyrolysis-Produced Tar Samples

sample	C	H	N	O[a]	S	H/C
tar (M1)	66.97	7.36	0.62	24.84	0.21	1.32
tar (M2)	67.63	7.17	0.63	24.36	0.21	1.27

[a]By difference.

The two pyrolysis processes were examined further to clarify these results. The differences in the opportunities provided for enabling the combination of the free-radical fragments generated by HLBE coal and the WSs are noteworthy here as well. In addition, the different environmental temperatures of WS pyrolysis in the two methods should be considered. In M1, the WSs were added to the reactor when the temperature of the HLBE coal sample was 400 °C; therefore, the volatiles generated from the WSs encountered an environmental temperature higher than 400 °C. However, in M2, the environmental temperature of the volatiles generated from the WSs was identical to the pyrolysis temperature and was below 400 °C. Therefore, the secondary reaction of the volatiles of the WSs was more significant[28] in M1, which led to the cracking of the long-chain aliphatic structures into short versions[29] and the generation of a greater number of small free radicals than that in M2. This was also confirmed by the higher compositions of the M1-generated hydrocarbon gases beyond 400 °C compared to those in M2 (Figure 4).

Essentially, the free-radical fragments of the WSs have more opportunities to combine with those from HLBE coal in M1, and the chain structures of the free-radical fragments of the WSs are shorter. Therefore, the combination of the free radicals from the WSs and HLBE coal in M1 stabilizes the free radicals and hinders the condensation of aromatic radicals produced during copyrolysis, leading to high levels of uncondensed aromatic hydrogen in tar. The short-chain structures of the volatiles concurrently lead to short side-chain structures in the tar.

2.3. Supply of WSs at Different Temperatures of HLBE Coal in M1. The M1-based experiments revealed that the simultaneous pyrolysis of different materials can be achieved to a certain extent, and a higher yield and quality of the copyrolysis-produced tar can be realized. However, the temperature of HLBE coal at which the WSs were fed to the reactor in M1, denoted as T_F, affects the "simultaneous" pyrolysis, which consequently influences the yield and

Table 2. Proton Distributions of Tar Generated by Copyrolysis

proton type (ppm)	assignments	M1	M2
H_{ar} (6–8.5)	**aromatic protons**	**22.6**	**21.8**
H_u (6–7.2)	uncondensed aromatic protons	16.5	12.1
H_c (7.2–8.5)	condensed aromatic protons	6.1	9.7
H_{al} (0.5–4.5)	**aliphatic protons**	**77.4**	**78.2**
H_γ (0.5–1.2)	protons of CH_3 in the γ position or further away from the aromatic ring	9.0	14.1
H_β (1.2–2.1)	protons of CH_2 or CH in the β position or further away from the aromatic ring; protons of CH_3 in the β position of the aromatic ring	20.7	24.7
H_α (2.1–4.5)	protons of CH, CH_2, or CH_3 in the α position of the aromatic ring	47.7	39.4

https://doi.org/10.1021/acsomega.1c06912
ACS Omega 2022, 7, 8717−8723

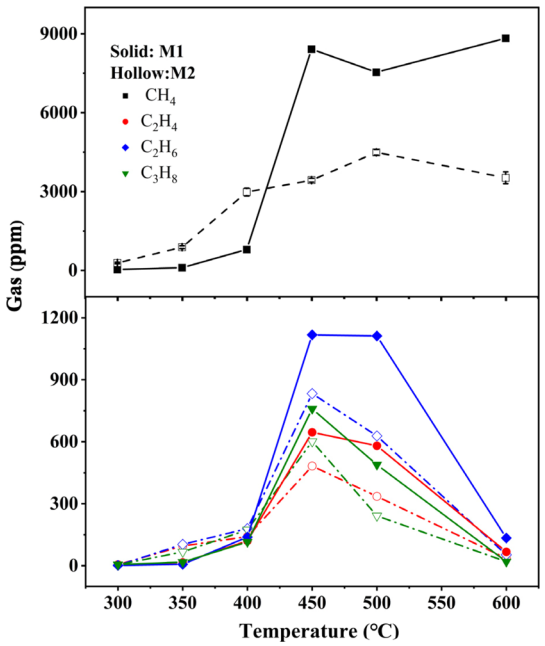

Figure 4. Compositions of the hydrocarbon gases.

properties of the tar. Figure 5a shows the yields of pyrolysis products obtained at T_F values of 300, 400, and 500 °C, which indicates that the char yields achieved at the different T_F values are nearly identical, and the gas yield increases with T_F. Moreover, the tar yield obtained at a T_F of 400 °C is the highest, and the water yield at this temperature is the lowest among the investigated samples. Figure 5b shows the free-radical concentrations of tar obtained at T_F values of 300, 400, and 500 °C (5.9×10^{16}, 3.7×10^{16}, and 4.9×10^{16} spins/g, respectively). These values are all lower than those of the M2-produced tar (7.2×10^{16} spins/g). The free-radical concentration of the tar produced at a T_F of 400 °C is the lowest, which indicates a low concentration of the heavy component and high quality of the tar. Therefore, Figure 5a,b suggests that the addition of biomass at the main pyrolysis temperature of coal can significantly improve the yield and quality of M1-produced oil.

The process of pyrolysis was further examined to interpret the results shown in Figure 5a,b. As mentioned earlier, the differences in the opportunities afforded for enabling combinations of the free radicals generated by the HLBE coal and WSs are relevant with respect to the different T_F values as well. As shown in Figure 2, the extent of coal pyrolysis is extremely small at 300 °C and almost complete at 500 °C; therefore, the binding reaction of the free radicals of HLBE coal and WSs is limited at T_F values of 300 and 500 °C. At a T_F of 400 °C, which is the main pyrolysis temperature of coal, the biomass and coal can realize "simultaneous" pyrolysis, and the free radicals of the two materials have more opportunities to combine with each other. Among the combination reactions, the combination of free radicals with $H^{\cdot}$ or $OH^{\cdot}$ may also lead to a decrease in the yield of water,[7] which is consistent with the experimental results. In addition, the environmental temperature of WS pyrolysis is different for the different values of T_F, and a higher environmental temperature leads to a higher degree of the secondary reaction of the volatiles, which increases the gas yield.

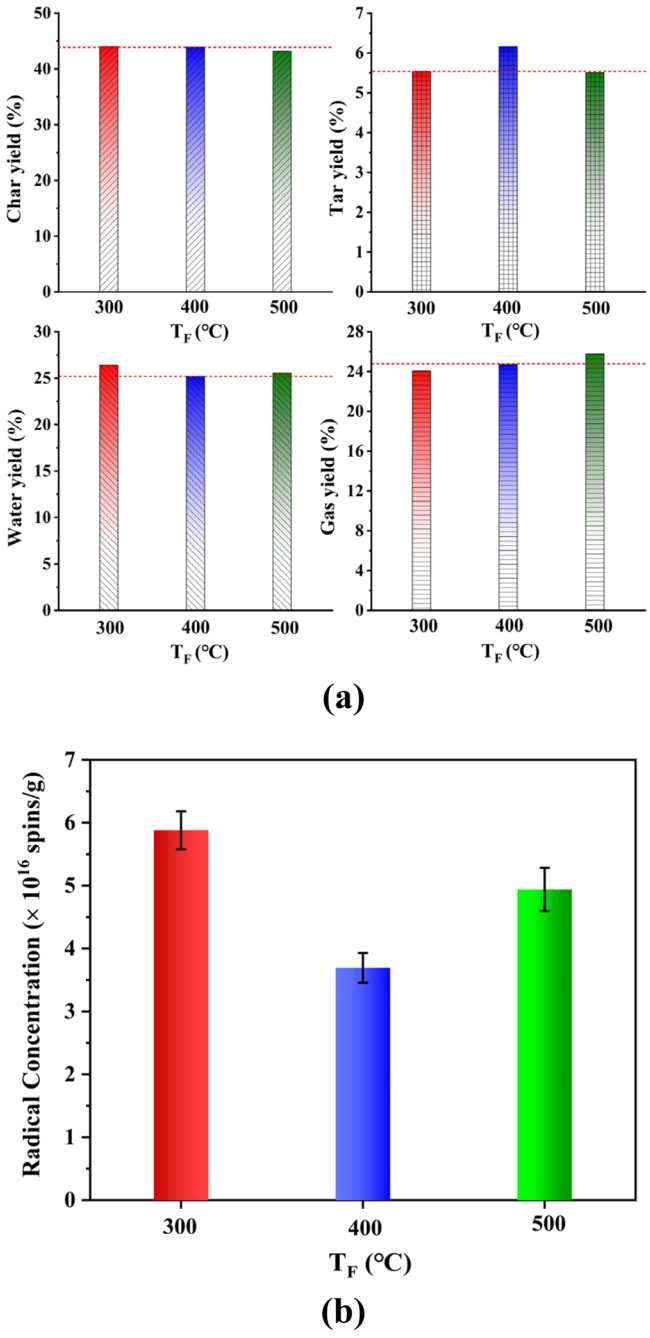

Figure 5. (a) Yields of pyrolysis products and (b) free-radical concentrations of tar samples obtained by M1 at T_F values of 300, 400, and 500 °C.

3. CONCLUSIONS

A new copyrolysis method (M1), which was developed to achieve "simultaneous" pyrolysis of coal and biomass, realized a higher tar yield and lower water content compared to those of M2, a fixed-bed-reactor-based method. The M1-produced tar exhibited a lower free-radical concentration, higher H/C ratio, higher concentration of uncondensed aromatic hydrogen, and shorter side-chains compared to those of M2, thereby demonstrating the synergistic effect in M1. The T_F affects the "simultaneous" pyrolysis and the synergistic effect in M1. The tar yield obtained at a T_F of 400 °C (the main pyrolysis temperature of coal) is the highest, the water yield is the lowest, and the free-radical concentration of the tar is also the

https://doi.org/10.1021/acsomega.1c06912
ACS Omega 2022, 7, 8717−8723

Table 3. Proximate and Ultimate Analyses of the Raw Materials[a]

	proximate analysis (wt %)				ultimate analysis (wt %)				
material	M_{ad}	A_{ad}	V_{ad}	FC_{ad}[b]	C_{daf}	H_{daf}	O_{daf}[b]	N_{daf}	S_{daf}
HLBE coal	22.96	9.54	31.54	35.96	74.21	3.05	20.91	1.3	0.53
WSs	9.84	2.79	66.69	20.68	53.12	3.15	42.44	0.93	0.36

[a]M: moisture; A: ash; V: volatile; FC: fixed carbon; *ad:* air dry; *daf*: dry and ash-free basis. [b]By difference.

lowest among the investigated samples, which indicated that the addition of biomass at the main pyrolysis temperature of coal produced oil with a superior yield and quality. These findings can enable improvements in the yields and properties of copyrolysis products.

4. EXPERIMENTAL SECTION

4.1. Materials. HLBE coal (lignite) and WSs (biomass) were used as raw materials. Proximate and ultimate analyses of these raw materials were conducted (Table 3). The HLBE coal and WSs were ground to 20−40 mesh sizes and subsequently dried under vacuum at 110 °C for 6 h prior to their use. Thermogravimetry (TG) analysis of the raw materials was performed using an STA 449 F3 (NETZSCH) TG analyzer.

4.2. Copyrolysis Experiments. Copyrolysis was conducted in a drop-tube−fixed-bed reactor (I.D., 34 mm; length, 300 mm), as shown in Figure 6. First, 2.5 g of HLBE coal was

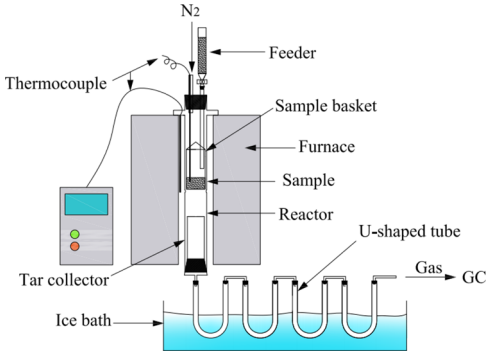

Figure 6. Schematic diagram of the copyrolysis reactor.

added to the sample basket of the reactor, following which pyrolysis was initiated at a heating rate of 5 °C/min and a nitrogen-gas flow rate of 200 mL/min. Subsequently, 2.5 g of WSs was added from the feeder when the temperature of the coal reached 400 °C. The experiment was terminated when the sample temperature reached 600 °C. This copyrolysis method is denoted as M1. A temperature of 600 °C in this experiment was chosen because the coal and biomass can be completely pyrolyzed at 600 °C, which can be seen from Figure 2.

The effects of supplying biomass at different coal temperatures on the yields and properties of the generated products were investigated by feeding the WSs into the reactor at HLBE coal temperatures of 300, 400, and 500 °C.

Copyrolysis was also performed in a fixed-bed reactor (M2), which was structured similar to the device shown in Figure 6 but without the feeder. First, 2.5 g each of the coal and biomass were simultaneously placed into the sample basket, with the coal being under the biomass. Pyrolysis was subsequently initiated at a heating rate of 5 °C/min and a nitrogen-gas flow rate of 200 mL/min. This experiment, which was denoted as M2, was terminated when the sample temperature reached 600 °C.

4.3. Yields and Properties of the Copyrolysis Products. The collection and calculation of the pyrolysis products have been thoroughly described in our previous report, and the reported maximum relative standard deviation of the product yield is 8.57%.[7] For the two pyrolysis methods, the collection and calculation of the pyrolysis products were the same and performed after the experiment. Here, we will state briefly. The amount of the char was obtained by measuring the masses of the sample basket before and after pyrolysis and was labeled as m_{char}. Most of the tar was collected from the tar collector, and the amount of the tar was calculated by subtraction and labeled as m_{tarC}. The uncondensed tar and water were cooled and collected in U-shaped tubes, and the amount of the uncondensed tar and water in the U-shaped tubes were calculated and labeled as m_{tarU} and m_{water} (details shown in reference 7).

The product yields were calculated by formulas 12345:

$$\text{Tar yield } (T) = \frac{m_{tarC} + m_{tarU}}{m_d(1 - A_d)} \quad (1)$$

$$\text{Char yield } (C) = \frac{m_{residue - mA_d}}{m_d(1 - A_d)} \quad (2)$$

$$\text{Water yield } (W) = \frac{m_{water}}{m_d(1 - A_d)} \quad (3)$$

$$A_d = \frac{A_{ad}}{1 - M_{ad}} \quad (4)$$

$$\text{Gas yield} = 1 - T - C - W \quad (5)$$

where m_d is the mass of the materials dried at 110 °C for 6 h, and d is the dry basis.

4.3.1. Determination of the Free-Radical Concentration. The free-radical concentrations of the resulting tar, which are known to reflect its quality and stability, were estimated by electron spin resonance (ESR; EMXnano, Bruker). The following test parameters were employed: microwave frequency, 9.6 GHz; microwave power, 0.3162 mW; central field, 3431.2 G; sweep width, 200.0 G; sweep time, 30.16 s; number of scans, 10; and modulation amplitude, 1.000 G. All ESR tests were performed at 25 °C, and the collected free-radical signals were subsequently integrated using Xenon software to automatically calculate the number of spins.

4.3.2. Proton Nuclear Magnetic Resonance Analysis of Tar. Five milligrams of the tar were placed in a nuclear magnetic resonance (NMR) tube and dissolved in 0.5 mL of DMSO-d. The ^{1}H-NMR spectrum was recorded at 15 °C using a Bruker Avance II 600 MHz spectrometer operating at 600.1 MHz. A total of 3072 scans were acquired at a relaxation delay of 2 s and an acquisition time of 1 s.

4.3.3. Gas Chromatography Analysis of Gaseous Products. Gaseous products, such as methane, ethane, ethylene, acetylene, and propane, were analyzed using a GC9790II setup with a flame ionization detector (FID) detector and a GDX-

https://doi.org/10.1021/acsomega.1c06912
ACS Omega 2022, 7, 8717−8723

502 column. The temperatures of the column box, injector, and FID were set at 40, 120, and 180 °C, respectively.

AUTHOR INFORMATION

Corresponding Authors

Wenjing He − *School of Environment and Chemical Engineering, Jiangsu Ocean University, Lianyungang, Jiangsu 222005, P. R. China;* orcid.org/0000-0002-9962-7078; Email: hewj@jou.edu.cn

Lanjun Zhang − *School of Environment and Chemical Engineering, Jiangsu Ocean University, Lianyungang, Jiangsu 222005, P. R. China*; Email: junjunzhang11@163.com

Authors

Yibo Zhao − *School of Environment and Chemical Engineering, Jiangsu Ocean University, Lianyungang, Jiangsu 222005, P. R. China;* orcid.org/0000-0001-9483-7933

Lu Chang − *School of Environment and Chemical Engineering, Jiangsu Ocean University, Lianyungang, Jiangsu 222005, P. R. China*

Tingting Huang − *School of Environment and Chemical Engineering, Jiangsu Ocean University, Lianyungang, Jiangsu 222005, P. R. China*

Guojun Yin − *Shandong Provincial Key Lab of Chemical Engineering and Process, Yantai University, Yantai, Shandong 264005, China;* orcid.org/0000-0001-8879-2142

Minjie Cui − *Institute of Physics and Beijing National Laboratory for Condensed Matter Physics, Chinese Academy of Sciences, Beijing 100190, China*

Shuyue Xu − *School of Environment and Chemical Engineering, Jiangsu Ocean University, Lianyungang, Jiangsu 222005, P. R. China*

Ziheng Liu − *School of Environment and Chemical Engineering, Jiangsu Ocean University, Lianyungang, Jiangsu 222005, P. R. China*

Complete contact information is available at: https://pubs.acs.org/10.1021/acsomega.1c06912

Notes

The authors declare no competing financial interest.

ACKNOWLEDGMENTS

This study was financially supported by the National Natural Science Foundation of China (21606095, 21606190, and 52004104), the Natural Science Foundation of the Jiangsu Higher Education Institutions of China (19KJB430012), the Natural Science Foundation of Jiangsu Province of China (BK20170452), and Jiangsu Province Graduate Research and Practice Innovation Project (KYCX20_2944, KYCX2021-041, and KYCX2021-003).

REFERENCES

(1) Soncini, R. M.; Means, N. C.; Weiland, N. T. Co-pyrolysis of low rank coals and biomass: product distributions. *Fuel* **2013**, *112*, 74−82.

(2) Li, J.; Zhu, J.; Hu, H.; Jin, L.; Wang, D.; Wang, G. Co-pyrolysis of Baiyinhua lignite and pine in an infrared-heated fixed bed to improve tar yield. *Fuel* **2020**, *272*, No. 117739.

(3) Zhang, L.; Xu, S.; Zhao, W.; Liu, S. Co-pyrolysis of biomass and coal in a free fall reactor. *Fuel* **2007**, *86*, 353−359.

(4) Park, D. K.; Kim, S. D.; Lee, S. H.; Lee, J. G. Co-pyrolysis characteristics of sawdust and coal blend in TGA and a fixed bed reactor. *Bioresour. Technol.* **2010**, *101*, 6151−6156.

(5) Wang, X.; Deng, S.; Tan, H.; Adeosun, A.; Vujanović, M.; Yang, F.; Duić, N. Synergetic effect of sewage sludge and biomass co-pyrolysis: a combined study in thermogravimetric analyzer and a fixed bed reactor. *Energy Convers. Manage.* **2016**, *118*, 399−405.

(6) Liu, M.; Yang, J.; Liu, Z.; He, W.; Liu, Q.; Li, Y.; Yang, Y. Cleavage of Covalent Bonds in the Pyrolysis of Lignin, Cellulose and Hemicellulose. *Energy Fuels* **2015**, *29*, 5773−5780.

(7) He, W.; Yin, G.; Zhao, Y.; Zhang, L.; Xu, S.; Huang, T.; Chang, L.; Lu, H. Interactions between free radicals during co-pyrolysis of lignite and biomass. *Fuel* **2021**, *302*, No. 121098.

(8) He, Q.; Guo, Q.; Umeki, K.; Ding, L.; Wang, F.; Yu, G. Soot formation during biomass gasification: A critical review. *Renew. Sustainable Energy Rev.* **2021**, *139*, No. 110710.

(9) Wu, Z.; Wang, S.; Zhao, J.; Chen, L.; Meng, H. Synergistic effect on thermal behavior during co-pyrolysis of lignocellulosic biomass model components blend with bituminous coal. *Bioresour. Technol.* **2014**, *169*, 220−228.

(10) Weiland, N. T.; Means, N. C.; Morreale, B. D. Product distributions from isothermal co-pyrolysis of coal and biomass. *Fuel* **2012**, *94*, 563−570.

(11) Moghtaderi, B.; Meesri, C.; Wall, T. F. Pyrolytic characteristics of blended coal and woody biomass. *Fuel* **2004**, *83*, 745−750.

(12) Sadhukhan, A. K.; Gupta, P.; Goyal, T.; Saha, R. K. Modelling of pyrolysis of coal−biomass blends using thermogravimetric analysis. *Bioresour. Technol.* **2008**, *99*, 8022−8026.

(13) Meng, H.; Wang, S.; Chen, L.; Wu, Z.; Zhao, J. Study on product distributions and char morphology during rapid co-pyrolysis of platanus wood and lignite in a drop tube fixed-bed reactor. *Bioresour. Technol.* **2016**, *209*, 273−281.

(14) Zhu, J.; Jin, L.; Luo, Y.; Hu, H.; Xiong, Y.; Wei, B.; Wang, D. Fast co-pyrolysis of a massive Naomaohu coal and cedar mixture using rapid infrared heating. *Energy Convers. Manage.* **2020**, *205*, No. 112442.

(15) Yuan, S.; Dai, Z.; Zhou, Z.; Chen, X.; Yu, G.; Wang, F. Rapid co-pyrolysis of rice straw and a bituminous coal in a high-frequency furnace and gasification of the residual char. *Bioresour. Technol.* **2012**, *109*, 188−197.

(16) Zhang, J.; Quan, C.; Qiu, Y.; Xu, S. Effect of char on co-pyrolysis of biomass and coal in a free fall reactor. *Fuel Process. Technol.* **2015**, *135*, 73−79.

(17) Quan, C.; Xu, S.; An, Y.; Liu, X. Co-pyrolysis of biomass and coal blend by TG and in a free fall reactor. *J. Therm. Anal. Calorim.* **2014**, *117*, 817−823.

(18) Ismail, T. M.; Banks, S.; Yang, Y.; Yang, H.; Chen, Y.; Bridgwater, A.; Ramzy, K.; Abd el-Salam, M. Coal and biomass co-pyrolysis in a fluidized-bed reactor: Numerical assessment of fuel type and blending conditions. *Fuel* **2020**, *275*, No. 118004.

(19) Wang, J.; Yan, Q.; Zhao, J.; Wang, Z.; Huang, J.; Gao, S.; Song, S.; Fang, Y. Fast co-pyrolysis of coal and biomass in a fluidized-bed reactor. *J. Therm. Anal. Calorim.* **2014**, *118*, 1663−1673.

(20) Sharifzadeh, M.; Sadeqzadeh, M.; Guo, M.; Borhani, T. N.; Murthy Konda, N. V. S. N.; Garcia, M. C.; Wang, L.; Hallett, J.; Shah, N. The multi-scale challenges of biomass fast pyrolysis and bio-oil upgrading: Review of the state of art and future research directions. *Prog. Energy Combust. Sci.* **2019**, *71*, 1−80.

(21) He, W.; Liu, Z.; Liu, Q.; Liu, M.; Guo, X.; Shi, L.; Wu, J.; Guo, X.; Ci, D. Analysis of Tars Produced in Pyrolysis of Four Coals under Various Conditions in a Viewpoint of Radicals. *Energy Fuels* **2015**, *29*, 3658−3663.

(22) He, W.; Liu, Q.; Shi, L.; Liu, Z.; Ci, D.; Lievens, C.; Guo, X.; Liu, M. Understanding the stability of pyrolysis tars from biomass in a view point of free radicals. *Bioresour. Technol.* **2014**, *156*, 372−375.

(23) Usmen, R.; Khan, R. Role of free radical chemistry on oxidative stability of coal pyrolysis liquids. *Fuel Process. Technol.* **1989**, *22*, 151−158.

(24) Dack, S. W.; Hobday, M. D.; Smith, T. D.; Pilbrow, J. R. Free radical involvement in the oxidation of Victorian brown coal. *Fuel* **1983**, *62*, 1510−1512.

(25) Wang, P.; Jin, L.; Liu, J.; Zhu, S.; Hu, H. Analysis of coal tar derived from pyrolysis at different atmospheres. *Fuel* **2013**, *104*, 14−21.

(26) Kapur, G. S.; Singh, A. P.; Sarpal, A. S. Determination of aromatics and naphthenes in straight run gasoline by 1H NMR spectroscopy. Part I. *Fuel* **2000**, *79*, 1023−1029.
(27) Yao, Q.; Kong, X.; Dai, X.; Gao, J.; Wang, R.; Zhang, Y.; Sun, M.; Ma, X. 1H NMR and 13C NMR characterization of n-heptane extraction of low-temperature coal tar reacted with formaldehyde. *Energy Sources, Part A* **2020**, *42*, 1490−1498.
(28) Liu, Z.; Guo, X.; Shi, L.; He, W.; Wu, J.; Liu, Q.; Liu, J. Reaction of volatiles−A crucial step in pyrolysis of coals. *Fuel* **2015**, *154*, 361−369.
(29) Dong, L.; Han, S.; Yu, W.; Lei, Z.; Kang, S.; Zhang, K.; Yan, J.; Li, Z.; Shui, H.; Wang, Z.; Ren, S.; Pan, C. Effect of volatile reactions on the yield and quality of tar from pyrolysis of Shenhua bituminous coal. *J. Anal. Appl. Pyrolysis* **2019**, *140*, 321−330.

https://doi.org/10.1021/acsomega.1c06912
ACS Omega 2022, 7, 8717−8723